

## Local and global ordering dynamics in multistate voter models

Lucía Ramirez<sup>1,2,\*</sup>, Maxi San Miguel<sup>1,†</sup> and Tobias Galla<sup>1,‡</sup>

<sup>1</sup>*Instituto de Física Interdisciplinar y Sistemas Complejos, IFISC (CSIC-UIB), Campus Universitat Illes Balears, E-07122 Palma de Mallorca, Spain*

<sup>2</sup>*Departamento de Física, Universidad Nacional de San Luis, Ejército de Los Andes 950, D5700HHW, San Luis, Argentina*



(Received 12 July 2022; accepted 14 October 2022; published 14 November 2022)

We investigate the time evolution of the density of active links and of the entropy of the distribution of agents among opinions in multistate voter models with all-to-all interaction and on uncorrelated networks. Individual realizations undergo a sequence of eliminations of opinions until consensus is reached. After each elimination the population remains in a metastable state. The density of active links and the entropy in these states varies from realization to realization. Making some simple assumptions we are able to analytically calculate the average density of active links and the average entropy in each of these states. We also show that, averaged over realizations, the density of active links decays exponentially, with a timescale set by the size and geometry of the graph, but independent of the initial number of opinion states. The decay of the average entropy is exponential only at long times when there are at most two opinions left in the population. Finally, we show how metastable states comprising only a subset of opinions can be artificially engineered by introducing precisely one zealot in each of the prevailing opinions.

DOI: [10.1103/PhysRevE.106.054307](https://doi.org/10.1103/PhysRevE.106.054307)

### I. INTRODUCTION

One of the most popular classes of models of opinion dynamics is that of so-called voter model (VM) [1–5]. VMs describe populations of individuals, who are each characterized by their discrete opinion state, and where the principal mechanism of change is imitation (i.e., one individual copies the opinion state of another individual). VMs are not only a paradigmatic model of opinion formation, they are also of interest in statistical physics. They operate out of equilibrium, and have absorbing states and certain symmetries, defining an interesting universality class [1,6].

In the most simple version of the VM each individual can take one of two opinion states. Individuals are assumed to reside on the nodes of an interaction network (this includes the special case of all-to-all interaction). At each step an individual is chosen at random and then copies the state of one randomly chosen neighbor on the network. This simple system has  $\mathbb{Z}_2$  symmetry, and two absorbing “consensus” states (if all individuals hold the same opinion, no further change is possible). The features of most interest to physicists include the time required to reach absorption, and the coarsening dynamics during the process leading to consensus [4–11].

Many variants of the voter model have been introduced in order to capture different features of social interaction. Examples are the so-called noisy voter model in which individuals can change opinion spontaneously [12–15], or populations including so-called “zealots.” These are individuals who are

less prone to changing opinion than regular agents, or who never change opinion [16–19]. A further variation, which we focus on here, is the so-called multistate voter model (MSVM) [20,21]. These are voter models in which there are more than two possible opinion states, and consequently multiple absorbing states. The path to one of these states involves a sequence of successive extinctions of opinions. One main distinction is between models in which the different opinion states are ordered in some way (representing, e.g., the political spectrum) versus models in which all states are equivalent. We here focus on the latter case.

Existing literature on MSVM with equivalent states includes in particular work on consensus and extinction times [20,22,23]. For the case of all-to-all interaction the authors of Ref. [20] derived analytical expressions for objects such as the mean consensus time, and the mean number of different states in the population as a function of time. Reference [20] also contains numerical studies of the model in low-dimensional lattices.

The authors of Ref. [22], among other results, further provided closed-form expressions for all moments of the consensus time for uniform initial distributions on the all-to-all interaction. Baxter *et al.* [23] obtain a solution for a model describing neutral genetic drift at a single locus with multiple alleles. This model, while set up in a biological context, is mathematically very similar to the MSVM in an all-to-all geometry, and the bulk of the ideas and results therefore carry over. It should be noted that the authors of [23] work in the diffusion approximation.

Many of the results in the existing literature concern quantities such as the consensus time, the time until the extinction of the different opinions, or the properties of the stationary state (the latter becomes nontrivial if spontaneous opinion

\*luciamirez@ifisc.uib-csic.es

†maxi@ifisc.uib-csic.es

‡tobias.galla@ifisc.uib-csic.es

changes are added to the dynamics, as this removes the absorbing states).

The question how consensus is reached in MSVMs, and what the coarsening process before absorption looks like, on the other hand, appear to have received relatively little attention. In this work, we therefore study the VM with a general number of initial opinion states, and with a focus on the dynamics before consensus is reached.

We focus on the cases of a complete graph (all-to-all interaction), uncorrelated networks such as Erdős-Rényi graphs, and scale-free networks [24]. Throughout our paper scale-free networks are generated using the Barabási-Albert growth process of preferential attachment [25] and have a degree distribution which decays as  $p(k) \sim k^{-3}$ . We will simply refer to these as Barabási-Albert networks

We focus on two key quantities in our analysis. One is the familiar “density of active links” [6,10–12,26–28], that is, the proportion of connected pairs of agents that do not share the same opinion. This quantity characterizes the organization of individuals on the graph. A low density of active links indicates the presence of domains of individuals of the same state (neighbors tend to be in the same opinion states). The pattern is more scattered if the density of active links is high [29]. Additionally, we look at the entropy of the distribution of agents across the different opinion states. This is a global measure of order (it does not make use of pairs of neighbors), indicating how dispersed the individuals are across the different opinions.

The time evolution of the density of active links in the two-state model has been studied on complete graphs [7,27] and on uncorrelated graphs [10–13,26]. Averaged over an ensemble of realizations, an exponential decay of the mean density of active links with time is here typically found. The decay time is proportional to the population size,  $N$ , for complete graphs and Erdős-Rényi networks [9,27]. On Barabási-Albert networks the timescale is proportional to  $N/\ln N$  [8].

The behavior in individual realizations is quite different. Both in the all-to-all scenario and on graphs one finds that single runs of the two-state VM typically settle to quasistable “plateau” of the density of active links, before a sudden fluctuation then takes the system to consensus [10,30]. The density of active links at the plateau differs in the cases of all-to-connectivity or networks. It also depends on the initial proportion of agents in the two opinion states [11].

In the two-state model consensus is reached after a single extinction of an opinion. The multistate model on the other hand undergoes a sequence of extinctions. Our main objective is to study how this affects the time evolution of the density of active links, and of the entropy. We address this both at the ensemble level (i.e., as an average over realizations) and on the level of individual runs.

The remainder of the paper is set out as follows. In Sec. II we define the model. Section III then focuses on the time evolution of the density of active links and of the entropy at the level of an ensemble average. The phenomenology of individual realizations is studied in more detail in Sec. IV. We find a sequence of metastable states and characterize some of the statistical features of these states. We then use this to establish how the ensemble-level behavior can be understood from that of single realizations. In Sec. V we then proceed

to show that zealots can be used to “engineer” steady states of mixed opinions similar to the metastable states found in individual realizations in Sec. IV. Finally, Sec. IV contains a summary and our conclusions.

## II. MODEL DEFINITIONS

### A. Setup and interaction network

The model describes  $N$  individuals, who can each be in one of  $M$  discrete states or opinions. We label individuals  $i = 1, \dots, N$  and states  $\alpha = 1, \dots, M$ . During the course of the dynamics each individual can interact with its nearest neighbors on a static network. We use the notation  $c_{ij}$  for the adjacency matrix of the undirected interaction network. We have  $c_{ij} = c_{ji} = 1$  if individuals  $i$  and  $j$  are neighbors, and  $c_{ij} = c_{ji} = 0$  otherwise. We also set  $c_{ii} = 0$ . We will use the notation  $j \in i$  to indicate that  $j$  is among the neighbors of  $i$ . We write  $k_i$  for the degree of the node representing individual  $i$ , i.e.,  $k_i = \sum_j c_{ij}$ . The total number of links in the graph is  $E = \sum_{i < j} c_{ij}$ . In the complete graph ( $c_{ij} = 1$  for all  $i \neq j$ ) one has  $E = N(N - 1)/2$ .

### B. Dynamics and transition rates

The variable  $s_i(t) \in \{1, \dots, M\}$  represents the state of individual  $i$  at time  $t$ . At the start of the dynamics ( $t = 0$ ) the states of all individuals  $s_i(t = 0)$  are initialized. Different initial conditions can here be chosen. We typically consider *homogeneous* initial conditions [20], that is a configuration in which the same number of agents in each opinion state are randomly distributed in the nodes of the network. For the model on networks, these individuals are placed on the graph at random.

The dynamics then proceeds through pairwise interactions between individuals. An interaction of individual  $i$  with individual  $j \in i$  consists of an imitation process, i.e.,  $i$  copies the opinion state of  $j$ . It is important to notice that, although the interaction network is undirected, each interaction event is directed. An interaction of  $i$  with  $j$  is not the same as an interaction of  $j$  with  $i$ .

The rates with which interactions between agent  $i$  and  $j$  occur are given by

$$T_{ij} = \frac{c_{ij}}{k_i} = \begin{cases} 1/k_i & j \in i \\ 0 & j \notin i. \end{cases} \quad (1)$$

In this setup time is continuous and measured in units of Monte Carlo steps (“generations” in the language of population dynamics), i.e.,  $O(N)$  imitation events take place in the population per unit time.

We denote the number of individuals holding opinion  $\alpha$  by  $n_\alpha$ , and we write  $\mathbf{n}(t) = [n_1(t), \dots, n_M(t)]$ . We also introduce  $x_\alpha = n_\alpha/N$  as the fraction of individuals in opinion state  $\alpha$ .

### C. Density of active links

At each point in time the links on the interaction network can be grouped into links that are “active” or “inactive” respectively. A link  $(i, j)$  is said to be active when the two nodes at its ends are in different states ( $s_i \neq s_j$ ), otherwise the link is inactive.

It is further useful to introduce the fraction of links of type  $\alpha\beta$ , where  $\alpha, \beta \in \{1, \dots, M\}$ . This is the fraction of links which have an agent in state  $\alpha$  at one end, and an agent in state  $\beta$  at the other end. Suppressing the time dependence of the  $\{i(t)\}$  we then have

$$\rho_{\alpha\beta} = \frac{1}{E} \sum_{i < j} c_{ij} (\delta_{s_i, \alpha} \delta_{s_j, \beta} + \delta_{s_j, \alpha} \delta_{s_i, \beta}) \quad (2)$$

for  $\alpha \neq \beta$ , and with  $\delta$  the Kronecker delta. We recall that  $E$  is the total number of links in the graph. The total density of active links in the system is then

$$\rho = \sum_{\alpha < \beta} \rho_{\alpha\beta} = \frac{1}{E} \sum_{i < j} c_{ij} (1 - \delta_{s_i, s_j}). \quad (3)$$

The overall rate of events in the population leading to state changes is proportional to the fraction of links that are active (an imitation process involving individuals connected by an inactive link will not result in any opinion change). The density of active links therefore characterizes the amount of (potential) ‘‘activity’’ and indicates how far the system is from reaching an absorbing state.

The density of active links can also be seen as a measure of disorder in the configuration of opinions on the interaction network. Consider a particular configuration  $\mathbf{n}$  of individuals in the different opinion states. If the individuals were located at random nodes on the graph with no particular order, then the probability that a randomly chosen link is active is  $\rho_{\text{random}} = 2 \sum_{\alpha < \beta} n_\alpha n_\beta / [N(N - 1)]$ . This is also the fraction of active links on a complete graph,  $\rho_{\text{CG}}(\mathbf{n})$ , given the  $\{n_\alpha\}$ . If there is order in the network (i.e., the neighbors of a node in state  $\alpha$  also tend to be in state  $\alpha$ ), then the density of links will be lower than  $\rho_{\text{CG}}(\mathbf{n})$ . At an absorbing state one has complete order,  $\rho = 0$ . Thus,  $\rho(\mathbf{n})$  indicates the amount of disorder in a configuration of the networked system. The behavior of this quantity in time can be used to characterize the coarsening dynamics. We stress that the density of active links arises from a local definition of disorder (the state of an individual is compared with that of its neighbors).

#### D. Entropy

We now introduce a second measure of disorder, namely, the entropy of a configuration of the system. This quantity relates to the distribution of individuals across opinion states in that configuration and is defined as

$$S = - \sum_{\alpha} x_{\alpha} \ln x_{\alpha}, \quad (4)$$

where we recall that  $x_{\alpha} = n_{\alpha}/N$ . No use of neighborhood relationships between nodes is here considered. Hence entropy as a measure of disorder has a global character. We stress that the entropy as defined in Eq. (4) can be evaluated (in simulations) at any time and for any specific realization. It therefore characterizes the global order in a particular snapshot of a simulation. This can then be averaged (at a fixed time) over realizations.

States of maximum entropy are those for which  $x_{\alpha} = 1/M$  for all  $\alpha$ , i.e., states with equally many individuals in each opinion state. This leads to  $S = \ln M$ . If the system has

reached consensus ( $x_{\alpha} = 1$  for one value of  $\alpha$ , and  $x_{\beta} = 0$  for all  $\beta \neq \alpha$ ), we have  $S = 0$ . This is the state of maximal order.

#### E. Master equation for the model on a complete graph

In an all-to-all geometry all individuals are equivalent in terms of their position on the graph, and the system is therefore fully specified by  $\mathbf{n} = (n_1, \dots, n_M)$ . The rates in Eq. (1) become  $T_{ij} = 1/(N - 1)$  for all  $i \neq j$ . This in turn means that the total rate with which individuals in state  $\alpha$  in the population are converted to individuals in state  $\beta$  is

$$\mathcal{T}_{\alpha \rightarrow \beta}(\mathbf{n}) = \frac{n_{\alpha} n_{\beta}}{N - 1}. \quad (5)$$

The dynamics of the system is then described by the master equation

$$\frac{d}{dt} P(\mathbf{n}) = \sum_{\alpha \neq \beta} (E_{\alpha} E_{\beta}^{-1} - 1) [\mathcal{T}_{\alpha \rightarrow \beta}(\mathbf{n}) P(\mathbf{n})], \quad (6)$$

where  $E_{\alpha}$  is the ‘‘raising operator’’ acting on functions of  $\mathbf{n}$  by increasing the argument  $n_{\alpha}$  by one,  $E_{\alpha} f(\mathbf{n}) = f(n_1, \dots, n_{\alpha} + 1, \dots, n_M)$ .

### III. CHARACTERIZATION OF THE COARSENING PROCESS AT THE LEVEL OF THE ENSEMBLE AVERAGE

To set the scene we will first focus on the time evolution of averaged quantities. By this we mean an average over realizations of the stochastic voter model dynamics, each realization with a different initial condition. We will refer to this as an ‘‘ensemble average’’ and use angle brackets  $\langle \dots \rangle$  to describe it. In numerical simulations we obtain this average from 5000 independent realizations.

#### A. Evolution of the average density of links

##### 1. Complete graph

In the basic case of all-to-all interactions one has, for any function  $f(\mathbf{n})$ ,

$$\frac{d}{dt} \langle f \rangle = \sum_{\mathbf{n}} f(\mathbf{n}) \frac{d}{dt} P(\mathbf{n}), \quad (7)$$

with  $\frac{d}{dt} P(\mathbf{n})$  as in Eq. (6).

From Eqs. (1) it is also clear that the rate for events converting individuals from state  $\alpha$  to state  $\beta$  is the same as that for the reverse event. Therefore, the ensemble average of  $x_{\alpha}$  is constant in time,

$$\frac{d}{dt} \langle x_{\alpha} \rangle = 0. \quad (8)$$

If an individual of type  $\alpha$  adopts opinion  $\beta$  in an event, then we have  $n_{\alpha} \rightarrow n_{\alpha} - 1$  and  $n_{\beta} \rightarrow n_{\beta} + 1$ . Given that  $\rho_{\alpha\beta} = 2n_{\alpha}n_{\beta}/[N(N - 1)]$  this means that  $\rho_{\alpha\beta}$  changes by  $2(n_{\alpha} - n_{\beta} - 1)/[N(N - 1)]$ . We therefore have

$$\begin{aligned} \frac{d}{dt} \langle \rho_{\alpha\beta} \rangle &= \frac{2}{N(N - 1)} \langle \mathcal{T}_{\alpha \rightarrow \beta}(\mathbf{n}) \times (n_{\alpha} - n_{\beta} - 1) \\ &\quad + \mathcal{T}_{\beta \rightarrow \alpha}(\mathbf{n}) \times (n_{\beta} - n_{\alpha} - 1) \rangle \\ &= - \frac{2}{N - 1} \langle \rho_{\alpha\beta} \rangle. \end{aligned} \quad (9)$$

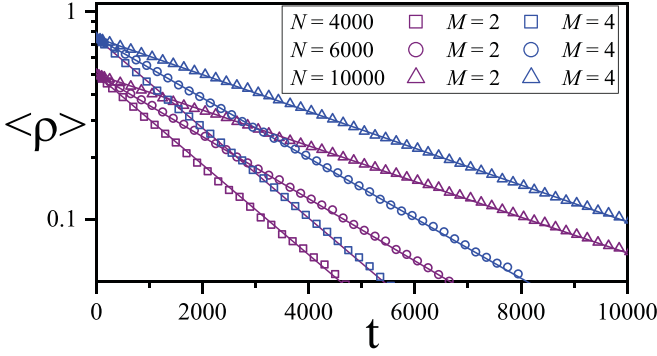


FIG. 1. Average density of links in the MSVM with all-to-all interaction and homogeneous initial conditions (see text) for different values of initial number of opinions  $M$  and different system sizes  $N$ . Symbols show results from numerical simulations, averaged over 5000 realizations. Lines are the analytical prediction in Eq. (12).

We conclude

$$\langle \rho_{\alpha\beta}(t) \rangle = \langle \rho_{\alpha\beta}(0) \rangle e^{-t/\tau}, \quad (10)$$

with a timescale  $\tau$  given by [27]

$$\tau = \frac{N-1}{2}. \quad (11)$$

From this and using Eq. (3) we have

$$\langle \rho \rangle = \langle \rho(0) \rangle e^{-t/\tau}. \quad (12)$$

We note that  $\tau$  is independent of the number of opinion states  $M$ .

For homogeneous initial conditions ( $n_\alpha = N/M$  for all  $\alpha$ ), we have

$$\langle \rho(0) \rangle = \frac{(M-1)N}{(N-1)M} \approx 1 - \frac{1}{M}, \quad (13)$$

where the approximation applies for  $N \gg 1$ .

In Fig. 1 we confirm the validity of Eq. (12) in simulations. The expression in Eq. (11) is verified in Fig. 2.

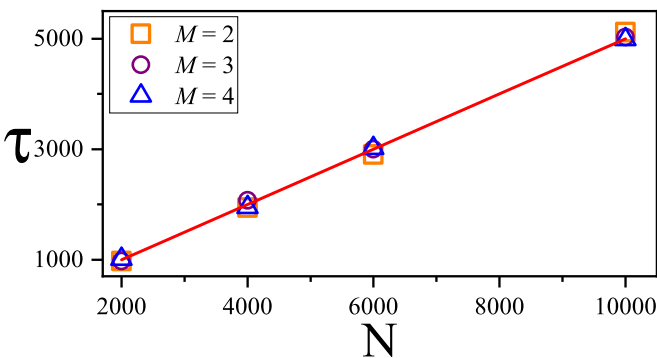


FIG. 2. Decay timescale  $\tau$  in the MSVM on a complete graph for different values of initial number of opinions  $M$ , as a function of the system size  $N$ . Markers are obtained from fitting an exponential curve to simulation data for  $\langle \rho(t) \rangle$ . The solid line shows Eq. (11).

## 2. Pair approximation for the two-state model on uncorrelated networks

In a networked geometry it is not straightforward to obtain closed laws for the time evolution of macroscopic average quantities such as the density of active links. This is because the state of the system is no longer fully described by the numbers  $n_1, \dots, n_M$ . The correlations that build up between nodes in the network are one key element distinguishing the voter process on networks from that with all-to-all interaction.

Analytical progress for the model on networks is possible as an approximation. One prominent approach is the so-called “pair approximation” [11,13,26,31], capturing correlations between nearest-neighbor nodes, but not between nodes which are further apart on the graph. The pair approximation is known to capture the behavior on uncorrelated networks to a good accuracy [11–13,26]. These networks can have an arbitrary degree distribution, but the degrees of nodes are uncorrelated, including the degrees of the nearest neighbor [32] (the probability that any two nodes are connected therefore depends only on their degrees). This includes Erdős-Rényi and Barabási-Albert networks.

Within the pair approximation the following expression can be found for the average density of active links in the VM with two opinion states [11,13]:

$$\langle \rho(t) \rangle = 2\langle x_1(0)[1-x_1(0)] \rangle \frac{\bar{k}-2}{\bar{k}-1} e^{-t/\tau} \text{ for } t > t^*, \quad (14)$$

where  $\bar{k}$  is the mean degree of nodes in the network. The quantity  $x_1(0)$  is the initial fraction of individuals in opinion state 1. If this fraction is fixed then the average  $\langle \dots \rangle$  on the right-hand side of Eq. (14) can be removed. Within the pair approximation the timescale  $\tau$  is given by [11]

$$\tau = \frac{(\bar{k}-1)\bar{k}^2 N}{2(\bar{k}-2)\bar{k}^2}. \quad (15)$$

In this expression,  $\bar{k}^2$  is the second moment of the degree distribution of the interaction network. A detailed derivation of Eqs. (14) and (15) can be found in [11].

It is important to note that Eq. (14) is valid only after a short transient of duration  $t^*$ . During this transient, the average density of active links reduces from its initial value  $2\langle x_1(0)[1-x_1(0)] \rangle$  by a factor of  $(\bar{k}-2)/(\bar{k}-1)$ . Unlike the decay time  $\tau$ , the timescale  $t^*$  does not increase with  $N$ , i.e., we have  $t^* = O(N^0)$  [11].

The time evolution of the average density of links in the two-state VM in Eq. (14) consists of three main factors: (1) the initial average density of active links,  $2\langle x_1(0)[1-x_2(0)] \rangle$ , one would obtain in an all-to-all geometry for the same distribution of initial proportions of agents in the two opinion states, (2) a factor  $(\bar{k}-2)/(\bar{k}-1)$  accounting for the network geometry, and (3) exponential decay.

## 3. Pair approximation for the MSVM

We will now use a simple argument to show that this general structure carries over to the multistate model. The only change required is to adapt the expression for the initial density of active links to the case of multiple opinion states, given initial proportions of agents in these different states.

The argument is based on the fact that the dynamics of one single opinion in the multistate voter model can be understood from a reduction to a two-state model. This was first proposed in the context of the VM in Ref. [5] and later used also in Ref. [14]. The same ideas can also be found in earlier work by Kimura and Littler in the field of genetics [33,34].

If the focus is on the dynamics of one single opinion (say,  $\alpha = 1$ ) then it is not necessary to resolve the different other opinion states. Instead what is relevant for an individual to change out of state  $\alpha = 1$  is that they interact with an individual in *any* of the other states. Similarly, an individual changes into state  $\alpha = 1$  if they were previously in any other state and interact with an individual in state 1. For the purposes of studying individuals in state  $\alpha = 1$  it is not required to know what these other states were. This means that all other opinions ( $\beta = 2, \dots, M$ ) can be amalgamated into one single opinion state. This then reduces the model to a two-state voter process: one state represents opinion  $\alpha = 1$  and the second state stands for “all other opinions.” We label these states as  $+$  and  $-$  respectively. The dynamical rules in Eq. (5) are such that this reduced models follows the dynamics of a two-state voter model.

Suppose now that we start the multistate voter process from homogeneous initial conditions,  $x_\alpha(0) = 1/M$  for  $\alpha = 1, \dots, M$ , and focus on a particular opinion. We then have  $x_+(0) = 1/M$ , and  $x_-(0) = 1 - 1/M$ . The reduced model is therefore a two-state voter model with inhomogeneous initial conditions.

Using Eq. (14) we have the following average density of active links in this reduced model,

$$\langle \rho_{\text{red}}(t) \rangle = 2 \frac{1}{M} \left( 1 - \frac{1}{M} \right) \frac{\bar{k} - 2}{\bar{k} - 1} e^{-t/\tau}. \quad (16)$$

We note that this is the average fraction of links between states  $+$  and  $-$  in the reduced model. In the original model (before the reduction) this corresponds to the fraction of links connecting an individual in state  $\alpha = 1$  with an individual in *any* other state  $\beta \neq 1$ , i.e.,  $\rho_{\text{red}} = \sum_{\beta > 1} \rho_{1,\beta}$ . Carrying out the ensemble average, and exploiting the symmetry between states in the MSVM with homogeneous initial conditions we have  $\langle \sum_{\beta > 1} \rho_{1,\beta} \rangle = \langle \sum_{\beta \neq \alpha} \rho_{\alpha,\beta} \rangle$  for any fixed  $\alpha$ . Hence, the resulting average density of active links in the MSVM is

$$\langle \rho(t) \rangle = \frac{1}{2} \sum_{\alpha \neq \beta} \langle \rho_{\alpha\beta}(t) \rangle = \frac{M}{2} \langle \rho_{\text{red}}(t) \rangle. \quad (17)$$

(In this expression both  $\alpha$  and  $\beta$  are summed over.) Using Eq. (16) we then obtain

$$\langle \rho(t) \rangle = \xi(M, \bar{k}) e^{-t/\tau} \text{ for } t > t^*, \quad (18)$$

with

$$\xi(M, \bar{k}) \equiv \left( 1 - \frac{1}{M} \right) \frac{\bar{k} - 2}{\bar{k} - 1}, \quad (19)$$

for the multistate voter model with homogeneous initial conditions. The decay time  $\tau$  is as in Eq. (15). As before, the exponential law in Eq. (18) is valid only after a short initial transient of duration  $t^* = O(N^0)$ .

Similar to the two-state model, we notice that the prefactor  $\xi(M, \bar{k})$  in Eq. (18) is made up of the network-specific factor

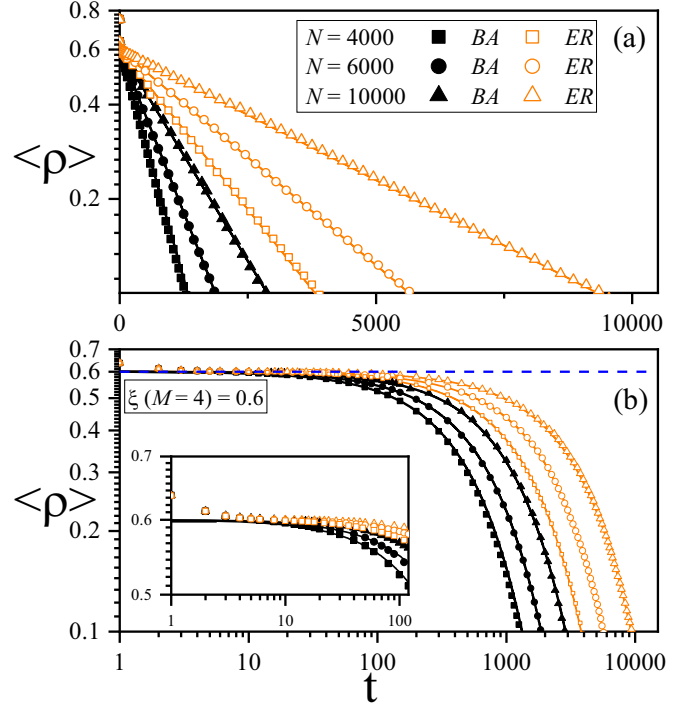


FIG. 3. (a) Time evolution of the average density of active links in the multistate voter model with  $M = 4$  for different systems sizes  $N$ . Markers show results from simulations, started from random homogeneous initial conditions, and averaged over 5000 realizations. We show data for Erdős-Rényi graphs (ER, orange open symbols) and for Barabási-Albert networks (BA, black full symbols). All networks have mean degree  $\bar{k} = 6$ . Solid lines are the analytical prediction in Eq. (18). Panel (a) is on linear-log scale. (b) The same data on double logarithmic scale, the density of active links shows a plateau  $\xi \approx 0.6$ , in line with Eq. (19). The lifetime of the plateau is finite for finite populations and increases with  $N$ . The inset provides a further zoom-in, highlighting the initial decay of the density of active links from its initial value to  $\xi = 0.6$ .

$(\bar{k} - 2)/(\bar{k} - 1)$ , and the density of active links  $1 - 1/M$  in Eq. (13), resulting from a configuration in which equally many individuals hold each opinion ( $x_\alpha = 1/M \forall \alpha$ ), and in which these individuals are placed on the network at random. The network-specific factor depends only on the mean degree.

#### 4. Test against simulations and metastable state in the coarsening dynamics

We now test the predictions of the previous section in numerical simulations. These were carried out on uncorrelated networks with different degree distributions, specifically the Erdős-Rényi and Barabási-Albert ensembles.

We first verify the validity of Eq. (18). We show the time evolution of the average density of active links,  $\langle \rho(t) \rangle$ , from simulations in Fig. 3, along with the analytical predictions from the pair approximation. As seen in the figure, satisfactory agreement is found. In Fig. 3(b) we replot the same data as in Fig. 3(a) but on a double logarithmic scale. This allows us to focus on the early stages of the time evolution. As also appreciated in the inset, the average density of active links

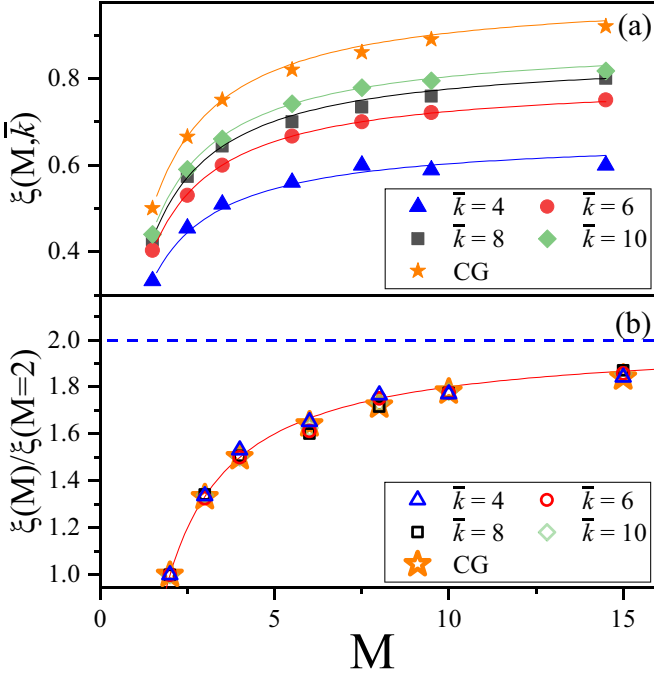


FIG. 4. (a) Density of active links,  $\xi(M, \bar{k})$ , in the metastable state as function of  $M$  for different values of  $\bar{k}$ . Markers show simulations with homogeneous initial conditions for the complete graph (CG, orange stars), and for Erdős-Rényi network with different mean degrees (the model on the Barabási-Albert network has the same plateau values as on Erdős-Rényi graphs). The data are obtained by measuring  $\langle \rho(t) \rangle$ , and then fitting to an exponential decay. Lines are from Eq. (19), shown also for noninteger values of  $M$  for optical convenience. Panel (b) shows  $\xi(M, \bar{k})/\xi(2, \bar{k})$  as function of  $M$ . Symbols are the simulations from (a); the solid line is Eq. (20).

$\langle \rho \rangle$  quickly decays to a value of  $\xi = 0.6$ , in line with the prediction of Eq. (19).

This initial decay of the density of active links is a signature of a rapid growth of local clusters of individuals with the same opinion state on the graph. As in the binary VM [11], this initial decay is not described by the exponential law for  $\langle \rho(t) \rangle$  from the pair approximation. After this initial phase the system is in a partially ordered metastable state, characterized by a density of active links  $\xi(M, \bar{k})$ . The system remains in this state indefinitely in the limit of infinite system size, we note that  $\tau \rightarrow \infty$  for  $N \rightarrow \infty$  in Eq. (15). If there are finitely many individuals in the network, then the system will eventually exit this state, triggered by fluctuations. Further ordering then occurs on a timescale of  $\tau$ , and the average density of active links decays exponentially.

We now make some further observations about the partially ordered state. As seen in Fig. 4(a), the density of active links in this initial metastable state,  $\xi(M, \bar{k})$ , increases with the mean degree of the network,  $\bar{k}$ , and with the number of opinion states,  $M$ . From Eq. (19) we find

$$\frac{\xi(M, \bar{k})}{\xi(2, \bar{k})} = 2 \left( 1 - \frac{1}{M} \right), \quad (20)$$

as confirmed in Fig. 4(b). We note the limiting value  $\xi(M, \bar{k})/\xi(2, \bar{k}) \rightarrow 2$  for  $M \rightarrow \infty$ .

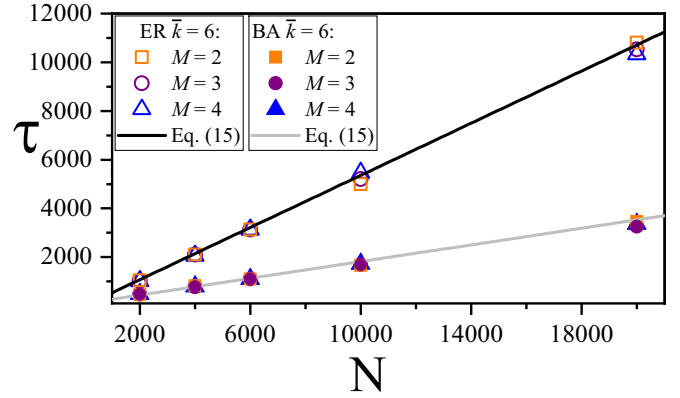


FIG. 5. Timescale  $\tau$  of the exponential decay of the average density of active links for Erdős-Rényi (ER) graphs (empty symbols) and Barabási-Albert (BA) networks (full symbols). The black and gray lines corresponds to Eq. (15) for ER ( $\bar{k} = 6$ ) and BA ( $\bar{k} = 6$ ), respectively. In line with Eq. (15)  $\tau$  is independent of  $M$ , i.e., the timescale  $\tau$  in the MSVM is identical to that in the two-state model. Simulation data are obtained from measuring  $\langle \rho(t) \rangle$ , and a subsequent fit to an exponential decay.

Finally, we briefly discuss the timescale  $\tau$  in Eq. (18), which is given by the expression in Eq. (15), and does not depend on the number of opinion states  $M$ . As such the timescale in the multistate model is the same as that in the conventional voter model with two opinion states. We note that the network structure enters not only through the mean degree  $\bar{k}$ , but also through the second moment  $\bar{k}^2$  of the degree distribution. As a consequence the exponential decay of  $\langle \rho(t) \rangle$  at fixed network size  $N$  and mean degree is slower on an Erdős-Rényi graph than on a Barabási-Albert network; see Figs. 3 and 5. As in the two-state model we have  $\tau \propto N$  for complete graphs and ER networks, but  $\tau \propto N/\ln N$  for large  $N$  in the BA network [8,10,11].

## B. Time evolution of average entropy

In numerical simulations we have also investigated the behavior of the average entropy,  $\langle S(t) \rangle = -\sum_{\alpha} \langle x_{\alpha} \ln x_{\alpha} \rangle$  over time. Simulation results are shown in Fig. 6. Inspection of our simulations shows that, at long times, the data are consistent with an exponential decay of the form

$$\langle S(t) \rangle = \xi_S(M, N) e^{-t/\tau}, \quad \text{for } t \gtrsim t_2; \quad (21)$$

see Fig. 6(a) and Fig. 7. The simulation data also indicate that the decay timescale  $\tau$  of this exponential decay at long times is the same as that for the average density of active links [e.g., Eq. (18)]. A theoretical argument for these observations is given below in Sec. IV C 2. The time  $t_2$  from which (approximately) the decay of the mean entropy becomes exponential can be estimated as the mean time at which only at most two opinions are left in the population. This time can be approximated analytically (see Sec. IV C below). When  $M = 10$ , we find  $t_2 \approx 0.38N$  for complete graphs, and  $t_2 \approx 0.07N$  on Barabási-Albert networks. These time points are indicated in Fig. 6(a). We stress that the deviations from an exponential for  $t \lesssim t_2$  are not short lived as those for the average density of

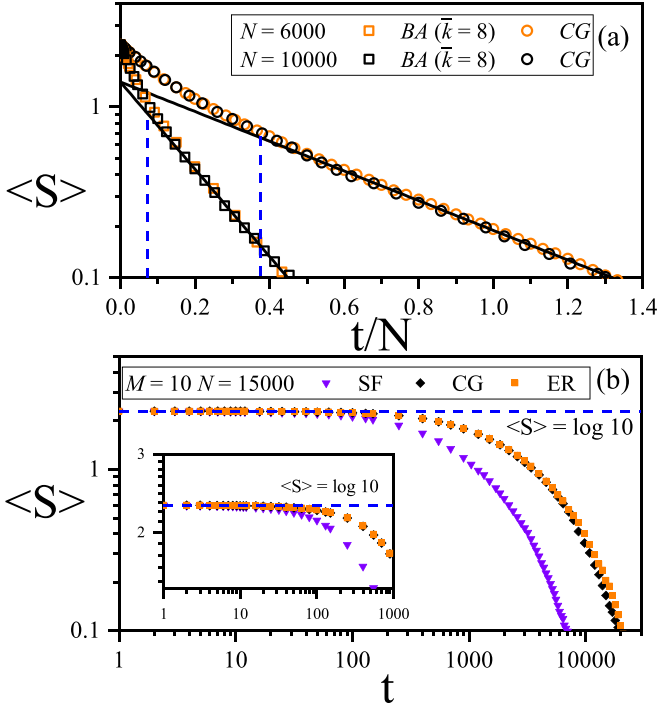


FIG. 6. Time evolution of the average entropy  $\langle S \rangle$  for a system started from homogeneous initial conditions and  $M = 10$ . Panel (a) shows results on complete graphs (CG) and on Barabási-Albert networks (BA, mean degree  $\bar{k} = 8$ ) on linear-log scale. Markers are from simulations (averaged over 5000 realizations). Lines are Eq. (21) with  $\tau$  given by Eq. (11) for the complete graph, and Eq. (15) for the BA networks. Vertical dashed lines indicate the time  $t_2$  beyond which there are typically at most two opinions present in the population (see Sec. IV C). Panel (b) shows  $\langle S \rangle$  on a doubly logarithmic scale for the CG (black diamonds), BA networks ( $\bar{k} = 8$ , purple triangles), and Erdős-Rényi graphs ( $\bar{k} = 8$ , orange squares), all for  $M = 10$  and system size  $N = 15000$ . The horizontal dashed line is  $S = S(t = 0) = \ln M$ . The inset shows a further zoom in, and highlights that on networks there is no short-time drop of the entropy from the initial value.

active links on networks. Instead we find that  $t_2$  scales linearly with the population size  $N$  . . .

Focusing on short times (of order  $N^0$ ) in Fig. 6(b) we note the absence of an initial drop of the mean entropy on networks. Instead the mean entropy remains at its initial value for homogeneous initial conditions,  $S(0) = \ln M$ . This is in contrast with the behavior of the average density of active links; compare with Fig. 3(b).

This suggests the following picture of the coarsening process on networks.

(1) Once released from the homogeneous initial condition the system first undergoes a quick local relaxation process during the time interval up to  $t = t^* = O(N^0)$ . In this phase the (average) density of active links reduces from its initial value  $1 - M^{-1}$  to the value  $\xi(M, \bar{k})$  given in Eq. (19). The average entropy however, remains unchanged,  $\langle S(t) \rangle = S(0) = \ln M$ . This indicates that during this phase some local ordering takes place on the network (hence the reduction in  $\langle \rho \rangle$ ), but that the proportions of individuals in the different opinion states do not materially change across the graph as a whole.

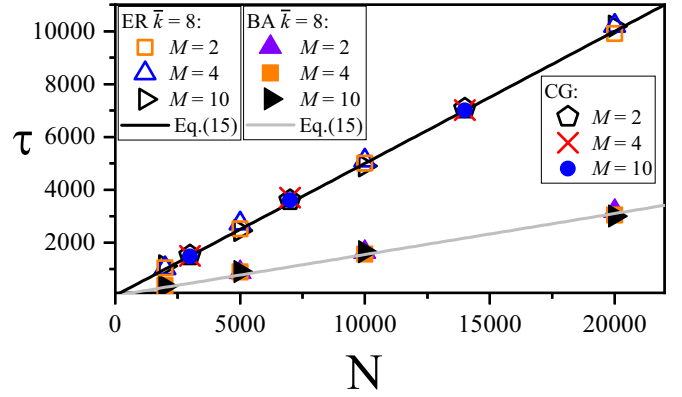


FIG. 7. Decay time of the average entropy for the complete graph (CG), and for Erdős-Rényi graphs (ER) and Barabási-Albert networks (BA) with mean degree  $\bar{k} = 8$  when, in average, there are two opinion states left. Markers are from fits of simulation data for  $\langle S(t) \rangle$  to an exponential at large times. The black solid line correspond to Eq. (15), evaluated for the ER graph where hence  $\tau \approx N/2$  for  $\bar{k} = 8$ , identical to the result for the complete graph. The gray line is from Eq. (15) evaluated for BA graphs with  $\bar{k} = 8$ .

One possible explanation is the formation of local domains. In each domain a particular opinion starts to outnumber the other opinion states. However, different domains do not “communicate,” hence the effects of the local ordering average out across the system.

(2) After this initial phase the system tends towards consensus, and  $\langle \rho(t) \rangle$  decays exponentially, with a timescale  $\tau = O(N)$ . The decay of the average entropy is not exponential until time  $t \approx t_2 = O(N)$ .

(3) At long times ( $t \gtrsim t_2$ ), when only two opinions are left in the system, the average entropy  $\langle S(t) \rangle$  also decays exponentially, on the same timescale  $\tau$  as the average density of active links.

We will discuss this further in Sec. IV C.

#### IV. PATH TO CONSENSUS IN INDIVIDUAL TRAJECTORIES

We now ask how representative the average behavior discussed in Sec. III is of the dynamics of individual realizations. We first focus on the density of active links, and subsequently study the entropy of the distribution of individuals across the different opinion states.

##### A. Evolution of the density of active links for individual realizations

###### 1. Sequence of plateaux in individual realizations

Figure 8 illustrates the time evolution of the density of active links for individual realizations of the model with  $M = 3$  opinion states on a complete graph [Fig. 8(a)] and on an Erdős-Rényi graph [Fig. 8(b)].

The density of links is first found to fluctuate around an initial plateau (on networks this is preceded by a short transient.) For the complete graph this plateau is located at a point consistent with the initial value of the density of active links for homogeneous initial conditions,  $\rho = 1 - M^{-1}$  [see

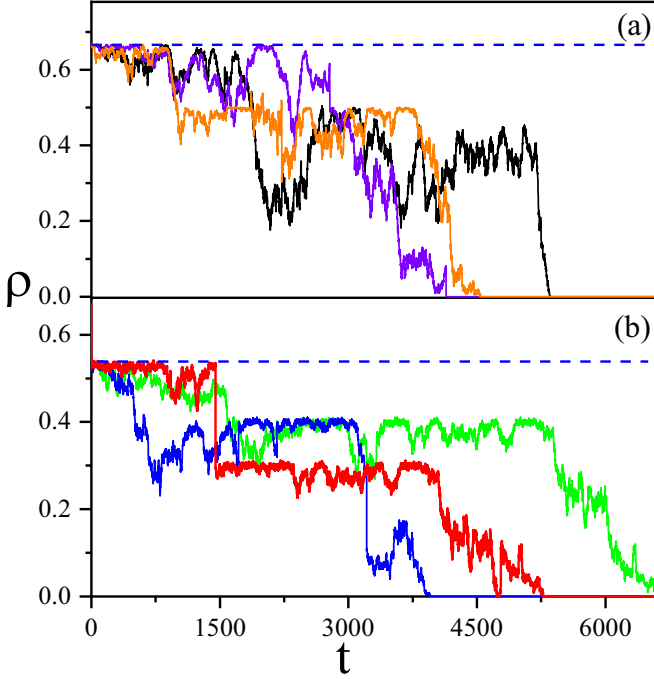


FIG. 8. Time evolution of the density of active links for three individual realizations indicated by different colors. Panel (a) is on a complete graph ( $M = 3, N = 6000$ ), panel (b) for an Erdős-Rényi graph ( $\bar{k} = 6, M = 3, N = 6000$ ). Simulations were started from homogeneous initial conditions. The dashed lines indicate the values obtained from Eq. (13) [ $\langle \rho(0) \rangle = 0.66$ ] and Eq. (19) [ $\xi(M = 3, \bar{k} = 6) = 0.66$ ], for the complete graph and Erdős-Rényi graphs, respectively.

Eq. (13)]. For the Erdős-Rényi network the density at this plateau is consistent with that predicted by Eq. (19).

Subsequently, the density of active links falls to a second plateau, where it then spends some time before a finite-size fluctuation takes the system to one of the absorbing states, where  $\rho = 0$ .

Unlike the initial plateau, the value of the density of active links at this second plateau differs from realization to realization (see Fig. 8). The process leading to this intermediate plateau can be better understood from the inspection of the evolution of the number of agents in each opinion state in Figs. 9(b) and 10(b). As shown, opinions go extinct one after the other. Each extinction takes the density of active links  $\rho$  to a new plateau (at a value lower than that of the previous plateau), until consensus is reached and  $\rho = 0$ .

When  $K$  extinctions have taken place in the model with initially  $M$  opinions, we are left with a MSVM with  $L = M - K$  states. Crucially, however, the initial condition for this model with  $L$  states is the result of the previous dynamics up to the time when the  $K$ th extinction takes place. This initial condition in turn determines the value of the density of active links at the subsequent plateau. Given that different realizations result in different configurations at the time of the extinctions the ensuing plateau densities also vary across realizations. This is the reason for the spread of plateaux in Fig. 8.

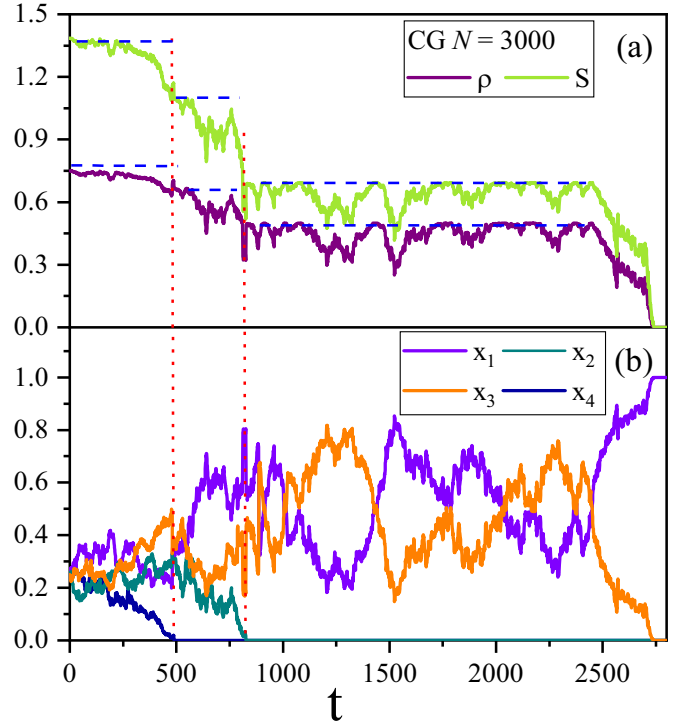


FIG. 9. (a) Evolution of the density of active links (purple curve), of the entropy (green curve) for the model on a complete graph. (b) The fraction of agents in each opinion state. Data are from a single simulation with  $M = 4$  and  $N = 3000$ . The vertical dotted lines indicate the points in time at which the first and second opinions go extinct respectively. Dashed lines represent the plateau value  $\xi$  considering a voter model with “4,” “3,” and “2” opinion states and the corresponding initial conditions; for the second and third plateaux, the value was computed considering the number of agents in the surviving opinions once the extinction of opinions “4” and “2” took place.

## 2. Density of active links at the different plateaux

We now proceed to calculate the mean density of active links in the model with initially  $M$  opinions at the first point in time where only  $L$  opinions are left. Suppressing any possible dependence on  $M$ , we will denote this quantity by  $\langle \rho \rangle_L$ .

Without loss of generality we assume that the  $L$  opinions left in the population are  $\alpha = 1, \dots, L$ . For an all-to-all interaction we then have

$$\rho = \frac{1}{2} \sum_{\alpha=1}^L [2x_{\alpha}(1-x_{\alpha})], \quad (22)$$

where  $\sum_{\alpha=1}^L x_{\alpha} = 1$ . Each term  $2x_{\alpha}(1-x_{\alpha})$  accounts for links involving individuals of type  $\alpha$  connected with individuals of any other opinion, and the overall prefactor  $1/2$  corrects for double counting. After taking an average over realizations we thus have

$$\langle \rho \rangle_L = \left\langle \sum_{\alpha=1}^L x_{\alpha}(1-x_{\alpha}) \right\rangle = L \int_0^1 dx P_L(x) x(1-x), \quad (23)$$

where the quantity  $P_L(x)$  is the distribution of the fraction of agents found in a particular opinion state when only  $L$

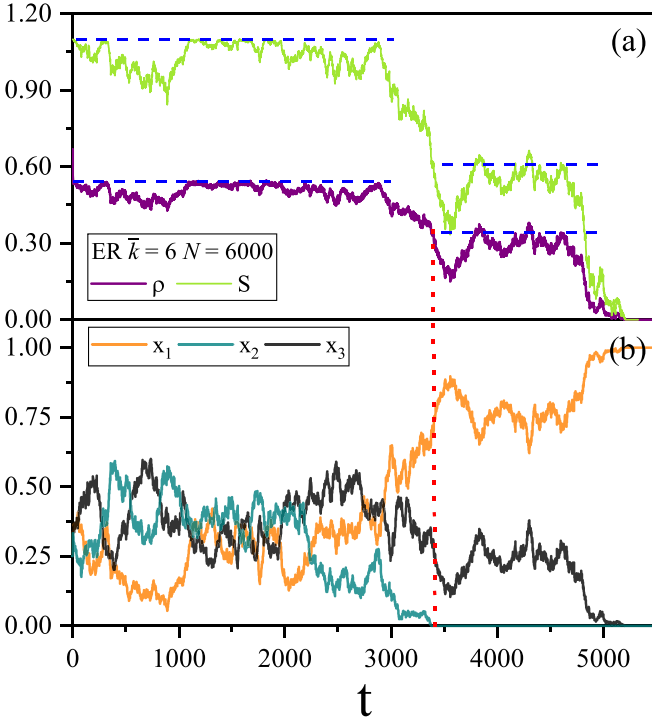


FIG. 10. (a) Evolution of the density of active links (purple curve) and of the entropy (green curve) for the model on Erdős-Rényi graphs. (b) The fraction of agents in the different opinion states. Data are from a single simulation with  $M = 3$  and  $N = 6000$ . The graph has mean degree  $\bar{k} = 6$ . The vertical dotted line indicates the time at which the first opinion state becomes extinct. Dashed lines represent the plateau value  $\xi$  considering a voter model with “3” and “2” opinion states and the corresponding initial conditions; the second plateau value was obtained considering the number of agents in the surviving opinions once opinion state “2” disappears.

opinions are left. We have used the fact that, by symmetry, no opinion state is preferred over any other.

The distribution  $P_L(x)$  can be obtained making the following hypothesis. We assume that, at the extinction point leaving only  $L$  opinions in the system, all configurations with  $x_\alpha \geq 0$  and  $\sum_{\alpha=1}^L x_\alpha = 1$  are equally likely, i.e., the distribution of  $(x_1, \dots, x_L)$  at that time is assumed to be

$$P_L(x_1, \dots, x_L) = [(L-1)!] \times \delta\left(\sum_{\alpha=1}^L x_\alpha - 1\right), \quad (24)$$

where  $\delta(\cdot)$  is the Dirac delta function.

The distribution  $P_L(x)$  in Eq. (23) is the single-variable marginal of  $P_L(x_1, \dots, x_L)$ ,

$$\begin{aligned} P_L(x_1) &= (L-1)! \int dx_2 \cdots dx_L \delta\left(\sum_{\alpha=1}^L x_\alpha - 1\right) \\ &= (L-1)(1-x_1)^{L-2}. \end{aligned} \quad (25)$$

For further details see Appendix A.

We can then directly calculate  $\langle \rho \rangle_L$  in Eq. (23),

$$\langle \rho \rangle_L = \frac{L-1}{L+1}. \quad (26)$$

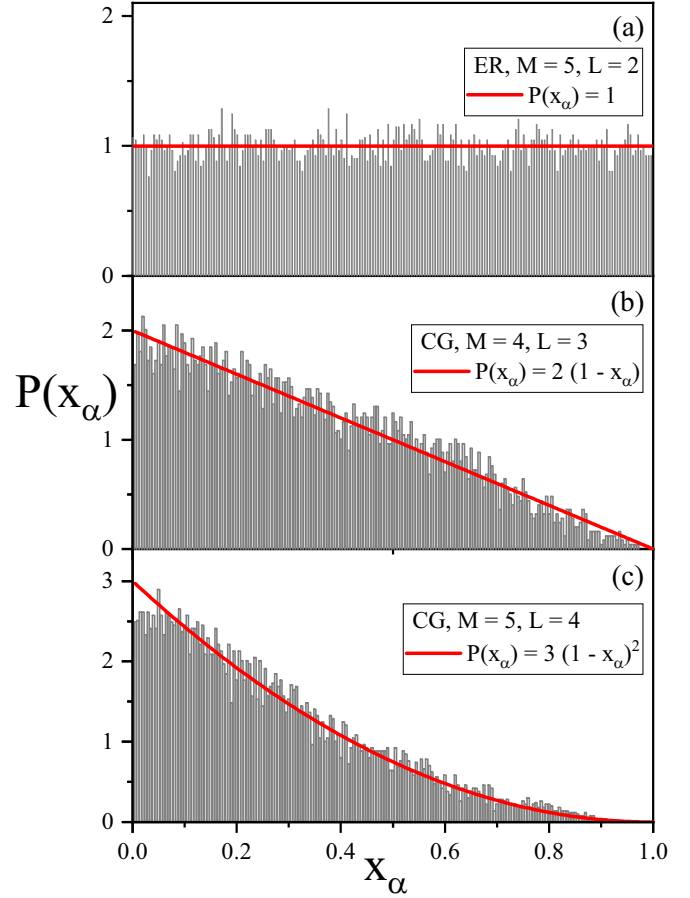


FIG. 11. Marginal distribution  $P_L(x_\alpha)$  for the fraction of agents in any one opinion at the first point in time when  $L$  opinions are left in a model with initially  $M > L$  states. Gray bars are from numerical simulations ( $N = 5000$ , averaged over 5000 realizations), the solid lines are Eq. (25). Panel (a) is for Erdős-Rényi networks, panels (b) and (c) for complete graphs.

The argument so far applies to complete graphs, where the initial condition is known to directly set the typical density of active links at the plateau that follows (see Sec. III). As also discussed in Sec. III, the system undergoes a brief transient when it is started on an uncorrelated graph, and the subsequent plateau value of  $\langle \rho \rangle$  is obtained applying a multiplication factor  $(\bar{k}-2)/(\bar{k}-1)$ . For uncorrelated graphs we therefore predict

$$\langle \rho \rangle_L = \frac{\bar{k} - 2L - 1}{\bar{k} - 1L + 1}. \quad (27)$$

### 3. Test against simulations

We now test these predictions against simulations. First, we verify the validity of our hypothesis of a flat distribution for  $(x_1, \dots, x_L)$  at the first point in time when there are only  $L$  opinions in the population. Figure 11 shows simulation results for the marginal distribution for  $x_\alpha$  for different choices of  $M$  and  $L$  on complete graphs and on Erdős-Rényi networks. As can be seen from the figure, these simulations are consistent with the predictions of Eq. (25).

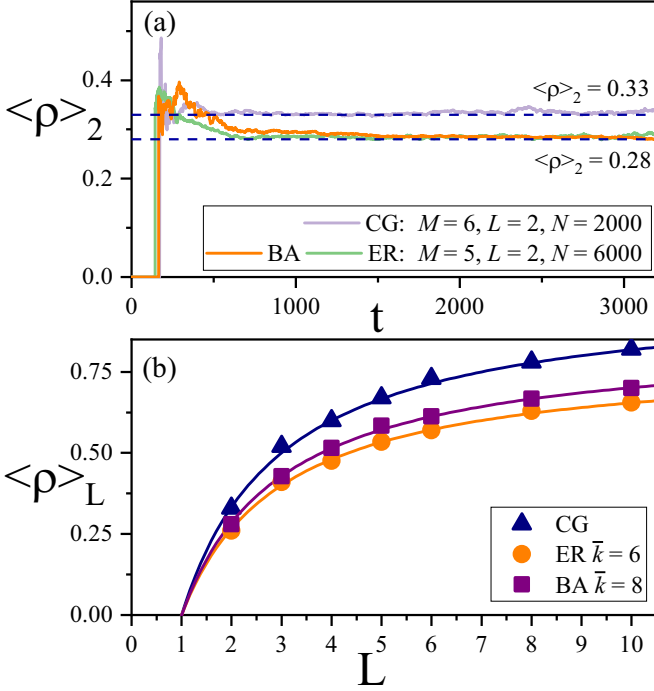


FIG. 12. (a) Evolution of the density of links in realizations for which only  $L = 2$  opinion states are left in the system for the CG, and the ER and BA networks with  $\bar{k} = 8$ . The plateau is located at  $\langle \rho \rangle_{L=2} \approx 0.33$  for the CG and at  $\langle \rho \rangle_{L=2} \approx 0.28$  for the networks, in good agreement with Eq. (26) and Eq. (27), respectively. (b) The location of the intermediate plateaux,  $\langle \rho \rangle_L$  as a function of  $L$  in a model with initially  $M = 15$  states. Markers are from simulations on CG (triangles), on BA networks (squares), and on ER networks (circles). Lines are from Eqs. (26) and (27) respectively.

We next introduce the concept of restricted ensemble at a given time. This is the ensemble of trajectories that, at this time, have precisely  $L$  surviving opinions. In Fig. 12 we show the average of the density of active links over this restricted ensemble. The data in Fig. 12(b) were obtained by first averaging over the restricted ensemble at any given time, and subsequently an average over time is performed. Figure 12(b) thus demonstrates that the average density of interfaces at the first point in time at which there are only  $L$  opinions in the system is given by Eqs. (26) and (27) for all-to-all interaction and on networks respectively, and that this average density of active interfaces is then maintained by the system until the next extinction occurs.

## B. Connection to exponential decay of the ensemble averaged density of links

### 1. Sequence of “jumps” in the model with multiple opinions

We have described the dynamics at the ensemble level and at the level of individual realizations. We now proceed to a characterization in terms of the restricted ensembles that we have just introduced.

The average density of active links,  $\langle \rho \rangle$  decays exponentially, as indicated in Eqs. (10) for complete graphs, and in Eq. (14) for uncorrelated networks. The decay timescales are given in Eqs. (11) and (15) respectively.

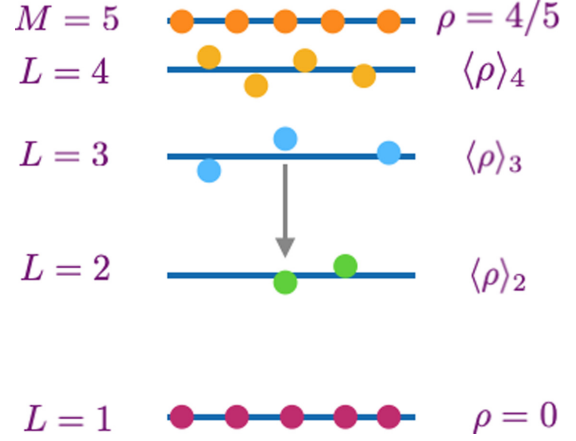


FIG. 13. Illustration of the jump process different realizations of the MSVM undergo. Each jump is associated with the extinction of one opinion. The density of active links in the resulting sequence of plateaux differs from realization to realization (as indicated by the scatter of markers), the mean density in the plateaux is given by Eqs. (26) or (27), respectively. In the final state ( $L = 1$ ) consensus has been reached, and hence  $\rho = 0$ . The residence time in each level varies from realization to realization as well, the mean time spent in level  $L$  is given by Eq. (29). The illustration is for a model with initially  $M = 5$  states. For homogeneous initial conditions one then has  $\rho = 4/5$ .

Individual realizations can be characterized as undergoing a sequence of “jumps” in the density of active links, from one plateau to another, as illustrated in Fig. 13. Each of these jumps is associated with the extinction of an opinion. As we have seen the density of active links along the sequence of plateaux differs across realizations. We have established that the average density of active links at the plateau at which  $L$  opinions are left in the population is given by Eq. (26) for complete graphs, and by Eq. (27) on uncorrelated networks.

### 2. Exponential decay in the ensemble on complete graphs

We would now like to connect the observations at ensemble level with those at the level of realizations. In order to do this we need information about the typical residence time in the different plateaux. We first discuss this for the model on the complete graph.

Following [20] the mean time the system spends in the metastable state with  $L$  opinions can be estimated as the difference between the mean consensus times in voter models with initially  $L$  or  $L - 1$  states respectively. The consensus time from a state with  $K$  opinions in the model with all-to-all interaction is given by [20]

$$\langle T_N(K) \rangle = N \frac{K-1}{K}, \quad (28)$$

for a system of size  $N$ , and assuming that all initial conditions are equally likely. We then have the following mean residence time in the state with exactly  $L$  opinions,

$$\langle \Delta t \rangle_L = \langle T_N(L) \rangle - \langle T_N(L-1) \rangle = \frac{N}{L(L-1)}. \quad (29)$$

We also know that the mean density of active links at the plateau with  $L$  opinions is  $\langle \rho \rangle_L = (L - 1)/(L + 1)$  [Eq. (26)]. Therefore the mean change of the density of links when transitioning from the plateau with  $L$  opinions to that with  $L - 1$  opinions is

$$\langle \Delta \rho \rangle_{L \rightarrow L-1} = \langle \rho \rangle_{L-1} - \langle \rho \rangle_L = \frac{-2}{L(L+1)}. \quad (30)$$

Using these results for  $\langle \Delta \rho \rangle_{L \rightarrow L-1}$ ,  $\langle \Delta t \rangle_L$  and  $\langle \rho \rangle_L$  we conclude

$$\frac{\langle \Delta \rho \rangle_{L \rightarrow L-1}}{\langle \Delta t \rangle_L} = -\frac{2}{N} \langle \rho \rangle_L. \quad (31)$$

The left-hand side is a proxy for the time derivative of  $\langle \rho \rangle$  when there are exactly  $L$  opinions in the system. The mean density of active links in this situation is  $\langle \rho \rangle_L$ . Therefore we have  $\frac{d}{dt} \langle \rho \rangle_L = -(2/N) \langle \rho \rangle_L$ , and we recover the exponential decay in Eq. (10). The timescale of the decay matches that in Eq. (11), up to the replacement  $N \rightarrow N - 1$  (which becomes irrelevant for large  $N$ ).

The exponential decay law [Eq. (12)] for the average density of active links in the ensemble can therefore be recovered from the picture of jumps in Fig. 13, and is a consequence of the specific relation between the level spacings and the mean residence time in each level.

### 3. Uncorrelated networks

A similar argument applies on uncorrelated networks. The  $\langle \rho \rangle_L$ , and hence the  $\langle \Delta \rho \rangle_{L \rightarrow L-1}$ , are then multiplied by the common factor  $(\bar{k} - 2)/(\bar{k} - 1)$ ; see Eq. (27). This therefore drops out in Eq. (31). In order to recover the exponential decay in Eq. (18) with a decay time as in Eq. (15) we then need to show that the result of [20] generalizes to uncorrelated graphs as follows:

$$\langle T_N(K) \rangle = N \frac{K-1}{K} \times \frac{(\bar{k}-1)\bar{k}^2}{(\bar{k}-2)\bar{k}^2}. \quad (32)$$

This can be demonstrated using a reduction to an effective two-state model, and the properties of the two-state VM on uncorrelated graphs, where it is known that the relevant timescales undergo rescaling by a factor  $[(\bar{k}-1)\bar{k}^2]/[(\bar{k}-2)\bar{k}^2]$  relative to the case of all-to-all connectivity [11]. This is described in more detail in Appendix B. The validity of Eq. (32) is demonstrated in Fig. 14.

### C. Evolution of the entropy for individual realizations and in the ensemble average

#### 1. Absence of simple exponential decay at ensemble level

In Figs. 9 and 10 we also observe intermediate plateaux in the time evolution of entropy for individual realizations. In Fig. 15(a) we therefore proceed as we did for the density of active links and perform averages over restricted ensembles of realizations with fixed  $L$  surviving opinions,  $L < M$ , at different times. In the example in the figure, we find that  $\langle S \rangle_{L=2} \approx 0.5$ .

Analytically, we find

$$\langle S \rangle_L = -L \int_0^1 dx P_L(x) x \ln x = H_L - 1, \quad (33)$$

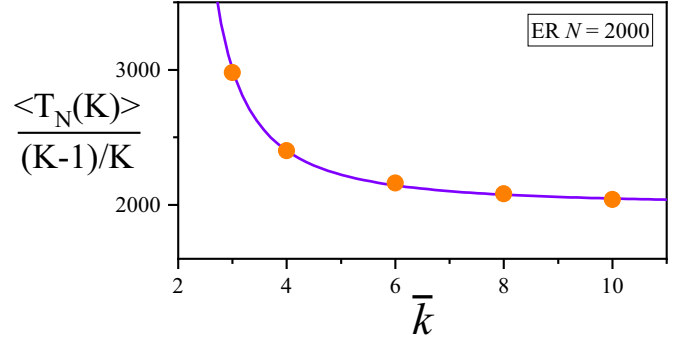


FIG. 14. Test of Eq. (32) for the model on Erdős-Rényi networks with  $N = 2000$ . Markers represent the ratio  $\langle T_N(K) \rangle / [(K - 1)/K]$  from simulations. The line is  $[(\bar{k} - 1)\bar{k}^2] / [(\bar{k} - 2)\bar{k}^2]$ , where  $\bar{k}^2 = Np(1 - p)$ , with  $p = \bar{k}/(N - 1)$ .

where the  $H_L = \sum_{\ell=1}^L (1/\ell)$  are the harmonic numbers. The distribution  $P_L(x)$  is given in Eq. (25). The prediction in Eq. (33) is tested against numerical simulations in Fig. 15(b).

We can now use this to understand in more detail why the decay of the entropy at ensemble level does not follow an

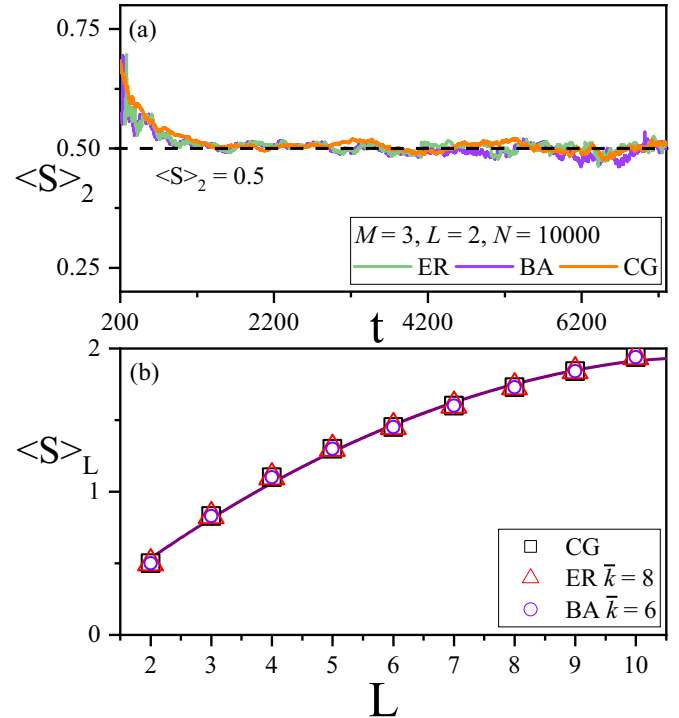


FIG. 15. (a) Time evolution of the entropy, at any time averages only over realizations for which exactly  $L = 2$  opinions are present in the population. Simulations are for the CG, ER, and BA graphs of size  $N = 10000$  and initially  $M = 3$  opinion states. The plateau is located at  $\langle S \rangle_L = 0.5$  in agreement with Eq. (33). (b) Symbols show simulation results for  $\langle S \rangle_L$  as a function of  $L$  in a model with initially  $M = 15$  opinions. Markers are from simulations for the CG (squares), ER graphs (triangles) and BA networks (circles). These are obtained from performing a time average on data such as the one in panel (a). The solid line is the analytical prediction in Eq. (33).

exponential law initially, but becomes exponential at long times. From Eq. (33) we find  $\langle \Delta S \rangle_{L \rightarrow L-1} = 1/L$ . Using Eq. (29) we then have

$$\frac{\langle \Delta S \rangle_{L \rightarrow L-1}}{\langle \Delta t \rangle_L} = -\frac{L-1}{N(H_L-1)} \langle S \rangle_L. \quad (34)$$

Interpreting the left-hand side again as a time derivative, we therefore have

$$\frac{d}{dt} \langle S \rangle = -\frac{1}{\tau_S(L)} \langle S \rangle \quad (35)$$

in the time regime when there are  $L$  opinions left in the system, with

$$\tau_S(L) = N \frac{H_L - 1}{L - 1} \quad (36)$$

for complete graphs, and  $\tau_S(L) = N \frac{H_{L-1}}{L-1} \times \frac{(\bar{k}-1)\bar{k}^2}{(\bar{k}-2)\bar{k}^2}$  on uncorrelated graphs.

The prefactor  $-1/\tau_S(L)$  on the right in Eq. (35) explicitly depends on  $L$ . In the corresponding equation (31) for the average density of active links the prefactor is instead constant. This is why the average density of links decays exponentially, and the average entropy does not. For  $L = 10$ ,  $\tau_S(L)$  evaluates to (approximately)  $0.21N$ , for  $L = 9$  to  $0.23N$ , for  $L = 8$  to  $0.25N$ , and so on. This demonstrates that the relative decay of the average entropy  $\langle S(t) \rangle$  slows down as more and more opinions become extinct.

We note that at any one time  $t$  different realizations of the MSVM process will be in states with different numbers of opinions  $L$  left in the population. It is therefore not straightforward to aggregate the mechanics of the decay of entropy for a fixed value of  $L$  [Eq. (35)] into a global picture for the behavior of entropy at the ensemble level. This is at variance with the decay of the average density of links. Given that all  $\tau_S(L)$  scale linearly in  $N$ , we can, however, conclude that all timescales governing the decay of entropy are  $O(N)$ , as also demonstrated in Fig. 6(a).

## 2. Regime at large times

One can identify a regime in which most realizations will either have reached consensus or in which the population contains only two opinions. In a model with initially  $M$  opinions this will be the case at times which are greater than

$$t_2 \equiv \sum_{L=3}^M \langle \Delta t \rangle_L. \quad (37)$$

This is the sum of average times spent in states with  $M, M-1, \dots, 3$  opinion states respectively, i.e., it is the mean time until only two opinion states are left in the system.

When  $L = 2$  opinions are left, we find  $\tau_S(L) = N/2$  for the complete graph in Eq. (36). In this long-time regime, we then have  $\frac{d}{dt} \langle S \rangle_2 = -(2/N) \langle S \rangle_2$ , leading to an exponential decay with the same timescale as that for the average density of active links. This provides a theoretical argument for the exponential law in Eq. (21) observed in numerical simulations. On uncorrelated networks this timescale is multiplied by the factor  $(\bar{k}-1)\bar{k}^2/[(\bar{k}-2)\bar{k}^2]$ .

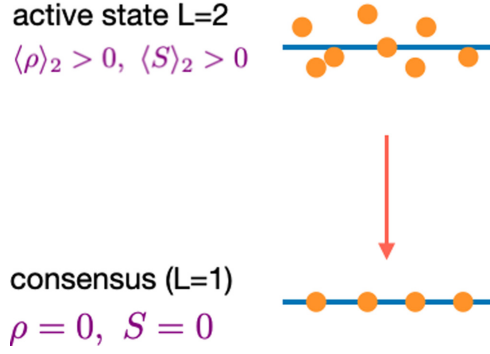


FIG. 16. Illustration of the dynamics when only at most two opinions are left in the population. Some realizations are in the active state (two opinions). Each such realization is in a metastable state with different plateau values for  $\rho$  and  $S$  across realizations. Transitions to consensus occur with rate  $\tau_S(L=2)^{-1} = 2/N$ , leading to exponential decay of  $\langle \rho \rangle$  and  $\langle S \rangle$  with a decay timescale  $N/2$ .

We can interpret this as the dynamics of a two-level system; see Fig. 16 for an illustration. Each realization will either have two opinions left in the population, or have reached consensus. There is hence an active state (two opinions) and a passive consensus state. Realizations in the active state have positive densities of active links and positive entropies. There is some scatter across realizations, and averages among active realizations are given by  $\langle \rho \rangle_2 > 0$  and  $\langle S \rangle_2 > 0$ , respectively. In the consensus state both  $\rho$  and  $S$  are zero. Each realization is first in the upper level ( $L = 2$ ), and then reaches consensus through a sudden fluctuation. This can be thought of as a Markovian jump process. Realizations transition from the upper to the lower level independently, with rate  $2/N$ . The population of the upper level hence decays exponentially in time. This then leads to the exponential decay of both  $\langle \rho \rangle$  and  $\langle S \rangle$ .

## V. STABILIZING INTERMEDIATE STATES THROUGH THE INTRODUCTION OF ZEALOTS

The sequence of plateaux discussed in previous sections is a consequence of long-lived metastable states in individual realizations. Eventually a finite system leaves each of these states, and proceeds to the next plateau and finally to absorption. In this section, we now seek to engineer a MSVM in which these intermediate states are stable indefinitely. We do this by adding zealots to the population, that is, agents who do not change their opinion state during the dynamics [17–19]. If such agents are added for more than one opinion state, then the system no longer has any absorbing states, and the dynamics continues indefinitely. The question we address here is if and how a configuration of zealots can be chosen so as to stabilize the metastable states in Sec. IV.

### A. Competing zealots

We consider a population of  $N$  conventional agents and  $Z$  zealots. As before  $n_\alpha$  is the number of agents in each opinion state  $\alpha = 1, 2, \dots, M$  (not including zealots). We write  $z_\alpha$  for the number of zealots for opinion state  $\alpha$ . Regular agents can

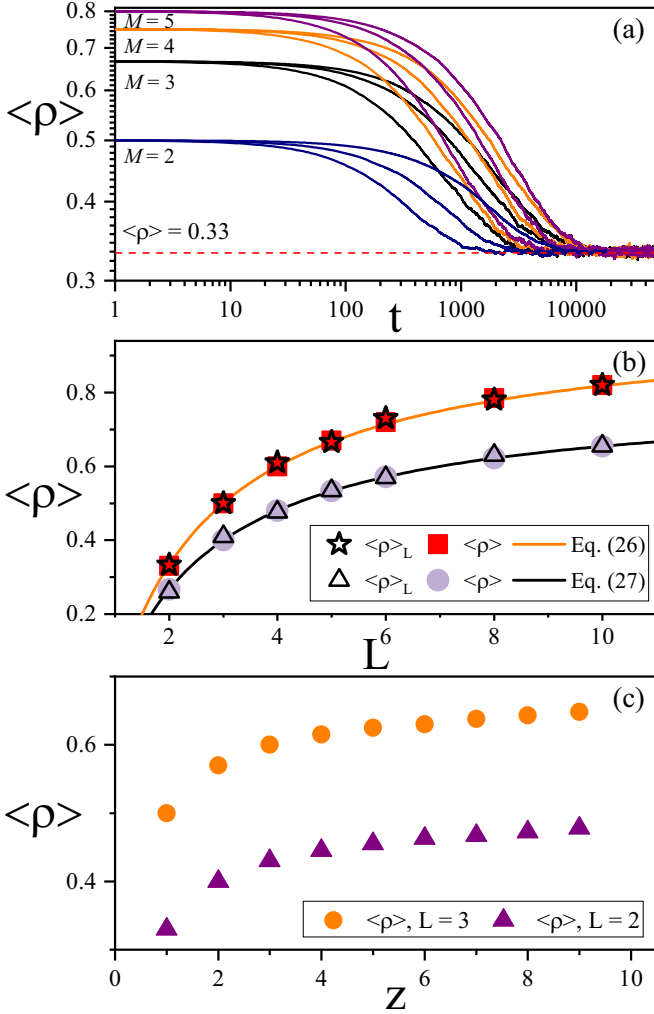


FIG. 17. (a) Time evolution of the average density of active links (complete graph) when there are two zealots of different opinions. At fixed number of opinions  $M$ , the size of the population was varied ( $N = 2000, 4000$ , and  $6000$ ). The horizontal dashed line indicates the value  $\langle \rho \rangle = 0.33$  obtained from setting  $L = 2$  in Eq. (26). (b) Filled symbols show the stationary density of active links,  $\langle \rho \rangle$ , in a model with one zealot in each of  $L$  different opinion states. Squares are for a complete graph, circles for ER networks. Open symbols show the density  $\langle \rho \rangle_L$  in a model with initially  $M = 15$  states (and no zealots). Stars are for a complete graph, triangles for ER networks. The lines are from Eqs. (26) and (27), respectively. (c) Simulation results for the stationary density of active links in a model with  $L$  opinions and  $z$  zealots in each of these opinions. Simulations are on complete graphs with system size  $N = 4000$ .

change their opinion by interacting with another regular agent or a zealot. Zealots never change their opinion.

We first focus on the model on a complete graph. The transition rates for this model are then

$$\mathcal{T}_{\alpha \rightarrow \beta} = \frac{n_{\alpha}(n_{\beta} + z_{\beta})}{N + Z}. \quad (38)$$

Suppose now, we start the VM with initially  $M$  states, and with two zealots of two different opinions. The remaining  $M - 2$  opinions will go extinct eventually. In Fig. 17(a) we

show the time evolution for  $\langle \rho \rangle$  for this system. The stationary density of active links is found as  $\langle \rho \rangle \approx 0.33$  in simulations, irrespective of the initial number of opinions  $M$ . This density of active links is consistent with that at the plateau for  $L = 2$  in the model without zealots in the previous section [Eq. (26)].

If, more generally, we populate  $L$  opinions with one zealot each, then, as seen in Fig. 17(b), the stationary density of active links also agrees with the plateau value  $\langle \rho \rangle_L$  in the model without zealots. This is found both on the complete graph and on uncorrelated networks.

The data in Fig. 17(c) show that the agreement in Figs. 17(a) and 17(b) between the density of active links of the model with one zealot in each of  $L$  opinions and the plateau  $\langle \rho \rangle_L$  in a zealot-free model with initially  $M > L$  opinions holds only when there is precisely one zealot in each of the  $L$  opinions. We further corroborate this in the next two subsections.

## B. Flat stationary distribution of opinions when there is one zealot in each opinion state

### 1. Analytical treatment of the model on a complete graph

We can demonstrate analytically that the stationary distribution [in the space  $(n_1, \dots, n_L)$ ] of the model with  $z$  zealots in each of  $L$  opinion states on the complete graph is flat if and only if  $z = 1$ . To do this we consider the master equation

$$\begin{aligned} \frac{dP(\mathbf{n})}{dt} = & \sum_{\alpha \neq \beta} P(n_{\alpha} + 1, n_{\beta} - 1) \frac{(n_{\alpha} + 1)(n_{\beta} - 1) + z}{N + Z} \\ & - \sum_{\alpha \neq \beta} P(\mathbf{n}) \frac{n_{\alpha}(n_{\beta} + z)}{N + Z}, \end{aligned} \quad (39)$$

where the notation  $P(n_{\alpha} + 1, n_{\beta} - 1)$  is a shorthand for  $P(E_{\alpha}E_{\beta}^{-1}\mathbf{n})$ , with the raising operator  $E_{\alpha}$  defined in Sec. II E. Direct algebra shows that  $P(\mathbf{n}) = \text{const.}$  is a stationary solution of Eq. (39) if and only if  $z = 1$ .

### 2. Numerical evidence for the model on networks

While an analytical solution for the model on networks is not easily available, simulation results are consistent with the assertion that placing one zealot in each opinion state leads to a flat stationary distribution in the space of  $(n_1, \dots, n_L)$ . We show the marginal stationary distribution  $P(x_{\alpha})$  for the model with  $z$  zealots in each of  $L$  opinions in Fig. 18. For  $z = 1$  these marginals are well described by the expression in Eq. (25), which is in turn derived from the assumption of a flat distribution  $P(x_1, \dots, x_L)$ . Figures 18(b), 18(d), and 18(f) on the other hand demonstrate that the marginals are markedly different when  $z \neq 1$ .

## VI. SUMMARY AND CONCLUSIONS

In summary, we have investigated the approach of multistate voter models to consensus. We have distinguished between the behavior of individual realizations and that of the ensemble average, and we have compared descriptions in terms of local and global properties. We have described local order by the density of active links, and global order by a time-dependent entropy. On networks, we find that local

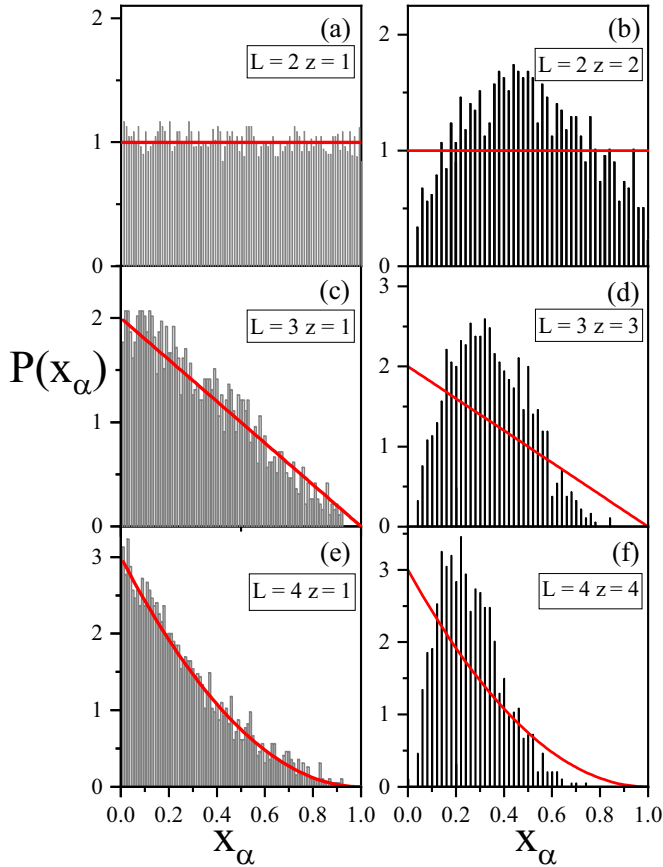


FIG. 18. Marginal distribution  $P_L(x_\alpha)$  for the fraction of agents in any one opinion for a MSVM with  $z$  zealots in each of  $L$  opinions. Gray bars are from numerical simulations for ER graphs of size  $N = 1000$  averaged over 5000 realizations. The solid lines are the prediction of Eq. (25), derived from the assumption of a flat stationary distribution.

ordering can occur without global ordering. There is an initial coarsening process up to a time  $t^*$ , in which the average density of active links decays to a value  $\xi(M, \bar{k})$  on networks, while the average entropy remains constant. The timescale  $t^*$  is independent of the size of the system. This initial decay is not observed in a complete graph where there is no distinction between local and global order.

At the level of an ensemble average, we further find that the density of active links decays exponentially after time  $t^*$ , with a time constant  $\tau$  which diverges with system size and which is independent of the number of initial opinions. This is observed both on complete graphs and on uncorrelated networks. As in the model with two opinion states, the amplitude and timescale of the exponential decay depend on the structure of the graph. The amplitude and the timescale can be characterized analytically using a pair approximation combined with a reduction to an effective two-state dynamics.

The behavior of the average entropy is more intricate. We find nonexponential behavior up to approximately the time at which only two opinions survive. For larger times the entropy decays exponentially with the same time constant  $\tau$  as the density of active links. All timescales associated with the

decay of the average entropy diverge with the system size. The timescale  $t^*$  (which is of order  $N^0$ ) has no particular significance for the average entropy. For large systems, the average entropy therefore remains at its initial value for very long times. On networks this is in contrast with the density of active links, which remains at a value associated with partial local ordering and which is lower than the initial density of active links.

Individual realizations undergo a sequence of extinctions of opinion states, akin to a “jump process.” We find that each realization remains in plateau values of the active links and entropy between successive extinctions. The location of these plateaux varies from realization to realization, and is determined by the configuration of the system at the time of the preceding extinction. The nonequilibrium ensemble average does not provide a proper description of this process, the individual realizations are not self-averaging.

To describe the ordering process we therefore introduce restricted ensembles of realizations which, at a fixed time, have a given number of surviving opinions. Averaging over these restricted ensembles in simulations allows us to study the mean plateau values exhibited by individual realizations. The average location of the plateaux can also be estimated analytically. The picture we develop is consistent with a maximum spread of configurations at the time of the intermediate extinctions. Using results from Ref. [20] for the mean time between extinctions we are also able to recover the exponential decay of the average density of active links from the jump process for individual realizations.

The restricted ensembles are a useful concept, and allow us to identify partially ordered states along the way to consensus. These states are very long lived in large populations, but eventually the system exits from these states. Arguably, the construction of these ensembles of realizations with  $L$  opinions in the system is also somewhat artificial. We have however shown that these partially ordered states can be engineered as genuine stationary states. This is achieved through the introduction of precisely one zealot in each of the  $L$  opinions.

In closing, we think that the combination of global and local measures of order provides an interesting way of looking at the coarsening dynamics in models of opinion formation. Our work also highlights that the time evolution of individual realizations can be very different from that of the ensemble average. Randomness can significantly influence individual trajectories, and the effects can last for substantial amounts of time. In other words, “history is contingent” [35]. The average path to consensus by opinion extinction is therefore of limited use for the description of a given historical empirical occurrence.

#### ACKNOWLEDGMENTS

We acknowledge support from Project APA-SOS reference PID2021-122256NB-C21 financed by MCIN/AEI/10.13039/501100011033 / FEDER, UE, and the Maria de Maeztu program for Units of Excellence in R&D (MDM-2017-0711) funded by MCIN/AEI/10.13039/501100011033. We acknowledge enlightening discussions with Raúl Toral.

**APPENDIX A: NORMALIZATION AND MARGINALS OF THE DISTRIBUTION  $P_L(x_1, \dots, x_L)$**

**1. Simplex in  $K$  dimensions**

For any  $K \in \mathbb{N}$  and  $y \geq 0$ , we define

$$\mathcal{S}_K(y) = \left\{ (x_1, \dots, x_K) : x_\alpha \geq 0, \sum_{\alpha=1}^K x_\alpha \leq y \right\}, \quad (\text{A1})$$

as the simplex of size  $y$  in  $K$  dimensions. We define its volume in  $K$  dimensions

$$V_K(y) = \int_{\mathcal{S}_K(y)} dx_1 \cdots dx_K, \quad (\text{A2})$$

and we have  $V_K(y) = y^K V_K(1)$  by simple scaling.

To evaluate  $V_K(1)$  we note

$$\begin{aligned} V_K(1) &= \int_0^1 dx_1 \int_{\mathcal{S}_{K-1}(1-x_1)} dx_2 \cdots dx_L \\ &= V_{K-1}(1) \int_0^1 dx_1 (1-x_1)^{K-1} \\ &= \frac{V_{K-1}(1)}{K}. \end{aligned} \quad (\text{A3})$$

We also have  $V_1(1) = 1$ . By induction therefore,  $V_K(1) = 1/K!$ , and

$$V_K(y) = \frac{y^K}{K!}. \quad (\text{A4})$$

**2. Normalization of  $P_L(x_1, \dots, x_L)$**

We start from the definition

$$P_L(x_1, \dots, x_L) = A \delta(x_1 + \dots + x_L - 1), \quad (\text{A5})$$

where the  $x_\alpha$  are required to be nonnegative, and where  $A$  is the appropriate normalization constant. Using  $\int dx_1 \cdots dx_L P_L(x_1, \dots, x_L) = 1$ , we have after integrating over  $x_L$ ,

$$A^{-1} = \int_{\mathcal{S}_{L-1}(1)} dx_1 \cdots dx_{L-1} = V_{L-1}(1) = \frac{1}{(L-1)!}. \quad (\text{A6})$$

Therefore,  $A = (L-1)!$ .

**3. Single-variable marginal of  $P_L(x_1, \dots, x_L)$**

We now calculate the single-variable marginal of  $P_L(x_1, \dots, x_L)$ ,

$$P_L(x_1) = \int dx_2 \cdots dx_L P_L(x_1, \dots, x_L). \quad (\text{A7})$$

Using the normalization constant in Eq. (A6) we have

$$\begin{aligned} P_L(x_1) &= (L-1)! \int dx_2 \cdots dx_L \delta(x_1 + x_2 + \dots + x_L - 1) \\ &= (L-1)! \int_{\mathcal{S}_{L-2}(1-x_1)} dx_2 \cdots dx_{L-1} \\ &= (L-1)! V_{L-2}(1-x_1). \end{aligned} \quad (\text{A8})$$

Hence, using Eq. (A4), we find

$$P_L(x_1) = (L-1)! \times V_{L-2}(1-x_1) = (L-1)(1-x_1)^{L-2}. \quad (\text{A9})$$

**APPENDIX B: EXTINCTION AND CONSENSUS TIMES IN ALL-TO-ALL GEOMETRIES AND ON GRAPHS**

In Sec. IV B we use a result for the average consensus time of the multistate voter model with  $K$  opinion states on an all-to-all geometry, and when initial conditions are chosen at random with flat distribution from the simplex defined by  $\sum_{\alpha=1}^L x_\alpha = 1$ . Specifically,

$$\langle T_N(L) \rangle = N \frac{L-1}{L}. \quad (\text{B1})$$

This was previously reported in Starnini *et al.* [20]. Starnini *et al.* derive this from the backward Fokker-Planck equation of the multistate model (valid in the limit of large, but finite  $N$ ), and using a separation ansatz exploiting the exchange symmetry between the different opinion states.

We use this consensus time to obtain the mean time,  $\langle t \rangle_{L \rightarrow L-1}$  that elapses in a model with initially  $L$  opinions until the first extinction, assuming again a uniform distribution of initial conditions in the simplex  $\sum_{\alpha=1}^L x_\alpha = 1$ .

The main purpose of this Appendix is to justify the generalization of the expression for the consensus time  $\langle T_N(L) \rangle$  to uncorrelated networks, Eq. (32). For convenience we repeat this expression here,

$$\langle T_N(L) \rangle = N \frac{L-1}{L} \times \frac{(\bar{k}-1)\bar{k}^2}{(\bar{k}-2)\bar{k}^2}. \quad (\text{B2})$$

Our argument is based on two principles. (1)  $\langle T_N(L) \rangle$  can be obtained from the so-called ‘‘mean conditional consensus time’’ of a suitable two-state model. This applies both in the case of all-to-all interactions and on networks. (2) The mean conditional consensus time for the two-state model in turn can be calculated (in the limit of large, but finite  $N$ ) from the backward Fokker-Planck equation (BFPE) of the respective model. It is known that the Fokker-Planck equation for the two-state model (and hence also the BFPE) on an uncorrelated network can be obtained from that for the model with all-to-all interactions by a rescaling of time by a factor of  $\frac{(\bar{k}-1)\bar{k}^2}{(\bar{k}-2)\bar{k}^2}$  [11]. This is also discussed in [8,9] although the factor is slightly different as explicitly acknowledged in [11].

We now address these two principles in turn.

**1. Reduction to two-state model**

Suppose the dynamics of the  $L$ -state model is started from an initial condition  $\mathbf{x} = (x_1, \dots, x_L)$  (with  $\sum_{\alpha} x_\alpha = 1$ ) at time  $t = 0$ . Writing  $p_C(\mathbf{x}, t)$  for the probability that consensus (on any opinion) has been reached by time  $t$ , we have

$$p_C(\mathbf{x}, t) = \sum_{\alpha=1}^L f_\alpha(\mathbf{x}, t), \quad (\text{B3})$$

where  $f_\alpha(\mathbf{x}, t)$  is the probability that consensus on opinion  $\alpha$  occurs by time  $t$ . We note that the events on the right in Eq. (B3) are all mutually exclusive.

The arrival time distribution at consensus (on any opinion) is then  $dp_C(\mathbf{x}, t)/dt$ , and the density of arrivals (per time) at consensus on opinion  $\alpha$  is  $df_\alpha(\mathbf{x}, t)/dt$ .

We note that

$$q_\alpha(\mathbf{x}) \equiv \int_0^\infty dt' f_\alpha(\mathbf{x}, t') \quad (\text{B4})$$

is the probability that consensus occurs in opinion  $\alpha$  (as opposed to another opinion). We have  $\sum_\alpha q_\alpha = 1$  (consensus occurs with certainty eventually), and in general  $q_\alpha < 1$  for any one opinion  $\alpha$  (i.e., the  $f_\alpha$  are not normalized probability densities).

We are interested in mean arrival times, so we calculate

$$\begin{aligned} \langle T_N(L, \mathbf{x}) \rangle &\equiv \int_0^\infty dt' t' \frac{d}{dt'} p_C(\mathbf{x}, t') \\ &= \sum_\alpha \int_0^\infty dt' t' \frac{d}{dt'} f_\alpha(\mathbf{x}, t'). \end{aligned} \quad (\text{B5})$$

This is the mean time to consensus (on any opinion). We have explicitly indicated the starting point  $\mathbf{x}$ . The average in this expression is only over realizations of the dynamics, but not over the starting point.

We next note that the mean consensus time, conditional on arrival at consensus on  $\alpha$ , is given by

$$\langle T_\alpha(\mathbf{x}) \rangle = \frac{\int_0^\infty dt' t' \frac{d}{dt'} f_\alpha(\mathbf{x}, t')}{q_\alpha(\mathbf{x})} \quad (\text{B6})$$

(we suppress the dependence on  $L$  and  $N$ ). Hence,

$$\langle T_N(L, \mathbf{x}) \rangle = \sum_\alpha q_\alpha(\mathbf{x}) \langle T_\alpha(\mathbf{x}) \rangle. \quad (\text{B7})$$

Consensus occurs at  $\alpha$  with probability  $q_\alpha(\mathbf{x})$ , and given  $\alpha$  the mean time for this consensus is  $\langle T_\alpha(\mathbf{x}) \rangle$ .

The key observation is now that, similar to the argument in Sec. III A 3,  $f_\alpha(\mathbf{x}, t)$  [and hence also  $q_\alpha(\mathbf{x})$ ] can be obtained from looking at a two-state version of the model, in which one opinion is  $\alpha$  and where all other opinions are amalgamated into one second opinion state. This idea was used in the context of the voter model in Ref. [5] and later in Ref. [14]. Similar principles had previously been proposed for multiallele models in the field of genetics [33,34].

We note that the above argument applies for all-to-all interaction and for networks. We did not make any assumptions on the interaction network in deriving any of the relations up to and including Eq. (B7). What does change in going from all-to-all interaction to networks is the functional form of object such as  $p_C(\mathbf{x}, t)$  and  $f_\alpha(\mathbf{x}, t)$ , but not the relations between these quantities.

*All-to-all interaction.* As an illustration we now show how the reduction to a two-state model can be used to calculate the mean conditional consensus times  $\langle T_\alpha(\mathbf{x}) \rangle$ , and from these, to derive Eq. (B1) (valid for all-to-all interactions).

If the two-state model is started with a proportion  $x$  of agents in opinion 1 (and  $1-x$  in opinion 2), then the mean consensus time conditioned on consensus in opinion 1 is

$$\langle T_1(x) \rangle = -N \frac{1-x}{x} \ln(1-x). \quad (\text{B8})$$

This is a well-known result; see, for example, [9].

Using this, and the reduction of the multistate model to the two-state model we then have

$$\langle T_\alpha(\mathbf{x}) \rangle = -N \frac{1-x_\alpha}{x_\alpha} \ln(1-x_\alpha). \quad (\text{B9})$$

We also note that  $q_\alpha(\mathbf{x}) = x_\alpha$  (this follows from the fact that the dynamics of the model preserves the time average  $\langle x_\alpha(t) \rangle$ ).

Hence, inserting into Eq. (B7),

$$\langle T_N(L, \mathbf{x}) \rangle = -N \sum_{\alpha=1}^L (1-x_\alpha) \ln(1-x_\alpha). \quad (\text{B10})$$

We next use this to derive Eq. (B1). To do this we need to average over  $\mathbf{x}$ , with a flat measure in the simplex defined by  $x_\alpha \geq 0$  and  $\sum_\alpha x_\alpha = 1$ . Exploiting the symmetry of the model we find from Eq. (B10),

$$\langle T_N(L) \rangle = -NL \int_0^1 dx P_L(x) (1-x) \ln(1-x), \quad (\text{B11})$$

with the marginal  $P_L(x) = (L-1)(1-x)^{L-2}$  in Eq. (25). Carrying out the integral we have

$$\langle T_N(L) \rangle = N \frac{L(L-1)}{L^2} = N \frac{L-1}{L}, \quad (\text{B12})$$

i.e., we recover Eq. (B1).

## 2. Extension to uncorrelated networks

We now discuss the extension of Eq. (B1) to uncorrelated networks, i.e., we derive Eq. (B2). All results apply in the pair approximation.

Based on the reduction argument in the previous section of this Appendix it is sufficient to show that the mean conditional consensus time of the two-state model in Eq. (B9) generalizes to

$$\langle T_\alpha(\mathbf{x}) \rangle = -N \frac{(\bar{k}-1)\bar{k}^2}{(\bar{k}-2)\bar{k}^2} \frac{1-x_\alpha}{x_\alpha} \ln(1-x_\alpha). \quad (\text{B13})$$

This time,  $\langle T_\alpha(\mathbf{x}) \rangle$ , in turn is derived from the backward Fokker-Planck equation describing the model in the limit of large, but finite  $N$ . This is standard in the case of all-to-all interaction (see, e.g., [9]).

The crucial observation is now that the (forward) Fokker-Planck equation of the two-state model on uncorrelated graphs is obtained from that for the two-state model with all-to-all interactions by a simple rescaling of time by a factor  $[(\bar{k}-1)\bar{k}^2]/[(\bar{k}-2)\bar{k}^2]$ . This is discussed in [11]; see, for example, Eq. (12) in this reference (see also [8,9]).

The same rescaling then also applies to the backward equation, and it then follows immediately that all timescales derived from the backward equation also undergo the same rescaling. This then leads to Eq. (B13).

- [1] T. M. Liggett, *Interacting Particle Systems*, (Springer, New York, 1985).
- [2] P. Clifford and A. Sudbury, *Biometrika* **60**, 581 (1973).
- [3] R. Holley and T. Liggett, *Ann. Probab.* **3**, 643 (1975).
- [4] C. Castellano, S. Fortunato, and V. Loreto, *Rev. Mod. Phys.* **81**, 591 (2009).
- [5] S. Redner, *C. R. Phys.* **20**, 275 (2019).
- [6] I. Dornic, H. Chaté, J. Chave, and H. Hinrichsen, *Phys. Rev. Lett.* **87**, 045701 (2001).
- [7] E. Ben-Naim, L. Frachebourg, and P. L. Krapivsky, *Phys. Rev. E* **53**, 3078 (1996).
- [8] V. Sood and S. Redner, *Phys. Rev. Lett.* **94**, 178701 (2005).
- [9] V. Sood, T. Antal, and S. Redner, *Phys. Rev. E* **77**, 041121 (2008).
- [10] K. Suchecki, V. M. Eguíluz, and M. San Miguel, *Phys. Rev. E* **72**, 036132 (2005).
- [11] F. Vazquez and V. M. Eguíluz, *New J. Phys.* **10**, 063011 (2008).
- [12] A. Carro, R. Toral, and M. San Miguel, *Sci. Rep.* **6**, 24775 (2016).
- [13] A. F. Peralta, A. Carro, M. San Miguel, and R. Toral, *Chaos* **28**, 075516 (2018).
- [14] F. Herrerías-Azcué and T. Galla, *Phys. Rev. E* **100**, 022304 (2019).
- [15] F. Vazquez, E. S. Loscar, and G. Baglietto, *Phys. Rev. E* **100**, 042301 (2019).
- [16] N. Khalil, M. San Miguel, and R. Toral, *Phys. Rev. E* **97**, 012310 (2018).
- [17] N. Khalil and T. Galla, *Phys. Rev. E* **103**, 012311 (2021).
- [18] M. Mobilia, *Phys. Rev. Lett.* **91**, 028701 (2003).
- [19] M. Mobilia, A. Petersen, and S. Redner, *J. Stat. Mech.* (2007) P08029.
- [20] M. Starnini, A. Baronchelli, and R. Pastor-Satorras, *J. Stat. Mech.* (2012) P10027.
- [21] G. Iannelli, G. De Marzo, and C. Castellano, *Chaos: Interdiscip. J. Nonlinear Sci.* **32**, 043103 (2022).
- [22] W. Pickering and C. Lim, *Phys. Rev. E* **93**, 032318 (2016).
- [23] G. J. Baxter, R. A. Blythe, and A. J. MacKane, *Math. Biosci.* **209**, 124 (2007).
- [24] Strictly speaking, the Barabási-Albert network is not free of degree-degree correlations [36,37]. However, these correlations are known to be small, and mostly limited to nodes with high degree in finite networks. The assumption of an uncorrelated network is then justified as an approximation [8,11].
- [25] A.-L. Barabási and R. Albert, *Science* **286**, 509 (1999).
- [26] E. Pugliese and C. Castellano, *Europhys. Lett.* **88**, 58004 (2009).
- [27] C. Castellano, V. Loreto, A. Barrat, F. Cecconi, and D. Parisi, *Phys. Rev. E* **71**, 066107 (2005).
- [28] C. Castellano, D. Vilone, and A. Vespignani, *Europhys. Lett.* **63**, 153 (2003).
- [29] H. Kauhanen, D. Gopal, T. Galla, and R. Bermúdez-Otero, *Sci. Adv.* **7**, eabe6540 (2021).
- [30] M. San Miguel, V. M. Eguíluz, R. Toral, and K. Klemm, *Comput. Sci. Eng.* **7**, 67 (2005).
- [31] R. Dickman, *Phys. Rev. A* **34**, 4246 (1986).
- [32] S. Dorogovtsev, *Phys. J.* **9**(11), 51 (2010).
- [33] R. A. Littler, *Math. Biosci.* **25**, 151 (1975).
- [34] M. Kimura, *Evolution* **9**, 419 (1955).
- [35] Z. D. Blount, R. E. Lenski, and J. B. Losos, *Science* **362**, eaam5979 (2018).
- [36] P. L. Krapivsky and S. Redner, *Phys. Rev. E* **63**, 066123 (2001).
- [37] R. Albert and A.-L. Barabási, *Rev. Mod. Phys.* **74**, 47 (2002).